International Journal of Emerging Technology and Advanced Engineering
Website: www.ijetae.com (ISSN 2250-2459, Volume 2, Issue 5, May 2012)

Vegetation Extraction from Free Google Earth Images of Deserts Using a Robust BPNN Approach in HSV Space

Mohamed H. Almeer

Computer Science & Engineering Department, Qatar University
Doha, QATAR
almeer@qu.edu.qa, almeerqatar@gmail.com

***Abstract*— The high resolution and span diversity of colored Google Earth images are the main reasons for developing a vegetation extraction mechanism based on BPNN (Back Propagation Neural Networks) that can work efficiently with poor color images. This paper introduces a method based on neural networks that can efficiently recognize vegetation and discriminate its zone from the desert, urban, and road-street zones that surround it. Our method utilizes a large number of training images extracted from 10's of images containing random samples from the same area of Google Earth. We then use the multi-layer perceptron, a type of supervised learning algorithm, to learn the relation between vegetation and desert areas based only on color. The proposed method was verified by experimentation on a real Google Images sequence taken for Qatar. Finally justified results were produced.**

***Keywords*— Remote sensing, neural networks, BPNN, digital image processing, classification, HSV color space.**

I. INTRODUCTION

Research efforts on the current global climate change crisis require that Earth's surface be assessed and monitored. Scientists started three decades ago to study and monitor vegetation using satellite remote sensing images. It has been shown that the information taken from these images is of great importance for managing natural resources. Vegetation provides a food source for living beings and plays essential roles in affecting global climate change. It can be seen that the variability of ecological change and other natural effects on the environment are caused by vegetation changes.

Vegetation mapping and classification also present valuable information to aid our understanding of the natural and manmade environments through quantifying vegetation cover at a given time point or over a continuous period. High priority has been given to acquiring updated data for vegetation cover changes frequently or annually to allow a better assessment of the environment and the ecosystem. Further, it is critical to obtain the current states of vegetation cover for an area of interest in order to initiate constructive environmental measures, such as vegetation protection and restoration, which leads to plant habitat conservation. Some of the general benefits of monitoring vegetation are that it provides an indication of ecological changes, estimations of desertification levels accumulated over time, an indication of water concentration in soils, and finally, identification of the effects of climate variability and other natural phenomena on the environment.

Qatar was in a stage of rapid development and growth during the 1970s and 1980s because of its increasing oil production, which tremendously boosted its economy. Qatar has now witnessed an appreciable expansion in agriculture, constituting a noticeable "agriculture biodiversity" that requires consideration. Thus, the monitoring of the coverage and spatial distribution of vegetation and agricultural areas of Qatar is becoming important to assist development studies.

Although the total land area of Qatar mostly comprises deserts, and its vegetation is closely related to its geography, geology, topography, soil type, and climate, some different vegetation zones can be found where trees, reeds, and shrubs, such as tamarind, phragmites, and mace (types of plantation), can grow. These regions are mostly to the east, near the coast. A few attempts have been made to monitor vegetation in Qatar relying solely on satellite imagery.

For efficient vegetation recognition, we need a robust algorithm that is effective despite the poor RGB colors of Google Earth and satisfies two requirements: robustness against confusion with other zones that are close in color, and the ability to learn from samples, improving its learning with the increase in samples.

International Journal of Emerging Technology and Advanced Engineering
Website: www.ijetae.com (ISSN 2250-2459, Volume 2, Issue 5, May 2012)

The usual RGB color system does not fulfill both of these requirements; however, a solution based on neural networks assisted by HSV/I (Hue, Saturation, and Value or Intensity) coloring can. Our method does not rely on assigning minimum and maximum color limit values for each category or class for recognition purposes but rather on collecting a large number of samples selected for each category as an indication of color variations. We selected images of urban areas, scattered farms, and loose desert vegetation as the target scope of this study.

Figure 1. Google Earth Images for different landscape of Qatar showing scattered and manmade vegetation

To classify each pixel into one of three zones, seven parameters related to the color of a target pixel and of its eight surrounding pixels were used: H value, S value, I value, mean of H values, standard deviation of H, mean of S values, and the standard deviation of S for the surrounding eight pixels. The H and S components were highly valued for their color categorization as they convey the origin of the real color, cancelling the effects of luminance and brightness. Luminance and brightness can differ according to the lightning environment. Fig. 2 shows the HSV coordinates for colors.

II. Related Works

In [1] and [2], the author presented a complete high-resolution aerial-image processing workflow for detecting and characterizing vegetation structures in highly dense urban areas. He depended on spectral indices and an SVM classifier.

Another article [3], although not directly related to satellite image analysis, treated the recognition of natural colors using computer-based algorithms. The author proposed improved color separation methods using fuzzy membership for feature implementation and ANN for feature classification. He applied an HLS color coordination system in a harness assembly recognition system. The ANN implementation was helpful in this study. In [4], the author used ANN multilayer perceptrons to detect street lane colors under several nonlinear changes in different illumination conditions. Although using the blue and green components of the ordinary RGB color coordinate system, he obtained excellent results in real-time driving conditions.

We have therefore decided to use ANN for the detection and classification processes and apply them on Google Earth free satellite images of the state of Qatar. The HSV subspace of a coloring system proved useful as it mimics the natural human vision process. The contribution of this study is two-fold. First, it increases the research done on vegetation detection for Qatar deserts, which at present is scarce, and second it uses the HSV coloring coordinate with BPNN for color separation and classification.

III. Vegetation Extraction

In the HSV color space, colors are specified by the components of hue, saturation, and value. We use the subspace of HSV/I (Hue, Saturation, and Intensity or Value) that is extracted from the RGB space. Conversion from RGB to HSV is performed in each pixel for all test images by

$$r = \frac{R}{255}, \quad g = \frac{G}{255}, \quad b = \frac{B}{255}$$

$$I = \frac{r + g + b}{3}$$

$$H = 90 - arctan\left(\frac{F}{\sqrt{3}}\right) \times \frac{180}{\pi} + \{0;\ g > b;\ 180 + g < b\}$$

$$F = \frac{2r - b - g}{g - b}$$

$$S = 1 - \frac{min(r, g, b)}{I}$$

The resultant value of H lies between [0, 1] after normalization. Hence, all three components of HSV will lie within the interval [0, 1].

International Journal of Emerging Technology and Advanced Engineering
Website: www.ijetae.com (ISSN 2250-2459, Volume 2, Issue 5, May 2012)

Since the H component is computed at angle intervals between 0° and 360°, the RGB space cube unit is mapped into a cylinder with height plus radius of length 1 as shown in the next figure.

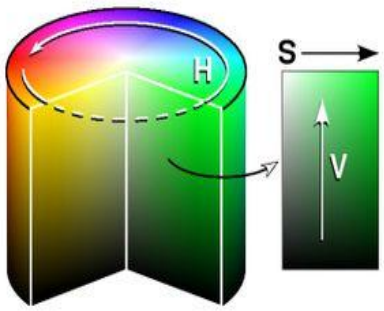

Figure 2. H-S-V Coloring coordinate

In contrast to the traditional representation, all HSV points within the cylinder correspond to valid RGB color coordinates. Mapping from RGB to HSV is non-linear.

IV. Google Earth

Google Earth is a popular free Internet application that provides a library of satellite imagery and aerial photography of the entire Earth's surface, thus supplying integrated coverage and monitoring images. Before high-resolution satellite imagery was developed, the availability of metadata was costly and scarce. However, the required satellite images are now free and offered on some sites and locations on the Internet, from which we chose Google as our study source. An obstacle to downloading high-resolution satellite images used to be the slow speed of data transfer. The images were also unavailable for the public. High-speed internet has made the process of downloading images much faster for ordinary users.

To enhance the appearance of Google Earth images, they are extensively processed in stages: color balancing, warping, and finally, mosaic processing. Google Earth images contain information from only three visible bands, so they are limited, especially in comparison with other satellite images such as those of "Landsat." Although this is a drawback, the images give excellent visual information of vegetation distribution in such a way that landmarks, vegetation, and shores are easily recognized.

For Qatar, the quality of images offered by Google Earth is quite good. They provide information on roads, vegetation, urban areas, and seashores. (See Figs. 1 and 3).

V. Desert-Road-Vegetation Color Problem

It is clear on inspection that in order to judge whether they belong to the desert or vegetation class, images collected from Google Earth require a supervised or non-supervised classification method based on pixel colors. Since the surrounding pixels surely give some indication concerning the nature of the target pixel, including these in the classification process makes it more accurate. We decided to use a supervised BPNN method because we considered it quite capable of efficient discrimination. For any supervised classification method, a large number of training samples is needed to achieve the best recognition results.

Another issue that emerged in the design phase was that of selecting the image from which to take the samples, and, in addition, having chosen an image, selecting the area from which the 20×20-pixel sample window should be extracted and saved for the training phase.

These particular questions were solved using a simple individual image inspection process based on a user's vision alone. Employing a highly trusted user to identify the required sub region in all the inspected images gave satisfactory results. The user selected approximately 20 to 25 20×20-pixel sub-images for each of the three classes to be used in the training phase. We inspected tens of Google Earth images of the desert surfaces of Qatar. Although simple in nature, this procedure showed excellent results for training as will be shown in the results and experimentation section. We tried to cover as many different areas as possible of the Qatar deserts where vegetation exists so that diversity would be guaranteed.

Fig. 3 shows some different vegetation scenes scattered across desert areas, on which the 20×20-pixel sample regions are imposed for clarity's sake. It also shows street and desert areas. The red and blue squares indicate the areas from which the sample region was taken, while the arrows indicate their different locations.

International Journal of Emerging Technology and Advanced Engineering
Website: www.ijetae.com (ISSN 2250-2459, Volume 2, Issue 5, May 2012)

Note that in the left image sample squares cover vegetation as well as desert surface, in the middle image sample squares cover only manmade vegetation, and finally in the right image sample squares cover both street and desert areas.

The HSV subspace is always considered because it gives truer color information, cancelling the effects of brightness, and is closer to real human recognition of colors than is the RGB subspace.

We therefore decided to implement the HSV coloring system. We particularly highly valued the H and S components after conversion from RGB, and relied on them as the two dominant properties for distinguishing land versus vegetation, as will be seen in next section.

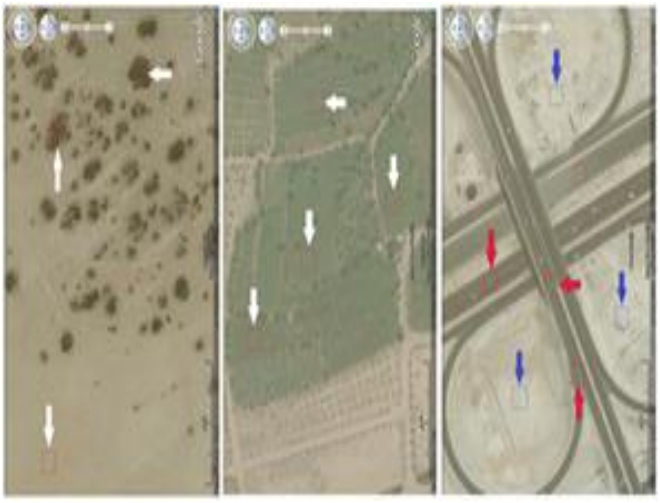

Figure 3. Sample extraction procedure from Google Earth images. The left image shows desert area with scattered vegetation; the sampled areas are indicated by white arrows. The middle image shows man-made vegetation. The right image shows streets landscape with some desert samples. Note that the red and blue squares show 20×20-pixel sample images.

All the collected regions are converted from the RGB color subspace to the HSV color subspace, pixel by pixel. As mentioned previously, we chose only two components of the HSV space, namely the H (Hue) and the S (Saturation) for each pixel and ignored the V (Value) component. Fig. 4 shows the distribution of all pixels in all training images when mapped into a 2-dimensional chart whose x-coordinate represents the Hue value [0, 1] and y-coordinate represents the Saturation value [0, 1].

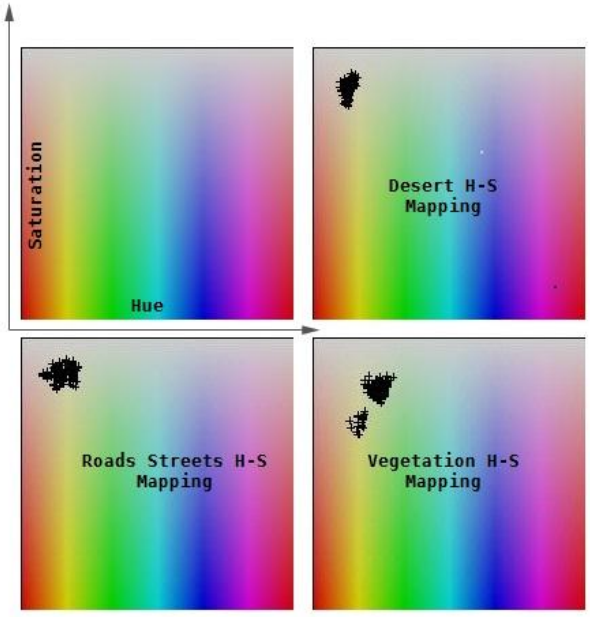

Figure 4. Hue-Saturation mapping for all the 20×20-pixel collected sample images of the three classes. Upper right shows Desert H-S mapping, lower left shows Road-Streets mapping, while lower right shows Vegetation mapping

From this chart, it can be seen clearly that the separation between Vegetation and Desert areas is clear, while the Road-Streets mapping is more deeply overlapped with Desert mapping. We therefore decided to combine the latter two classes into one, called the Desert-Street-Road class. Other mapping functions may be able to discriminate between desert and street by color, relying on other coordinates. However, for our study, it was sufficient to separate the colors of vegetation from all others. Our motivation was our intention to focus on extracting vegetation from other different classes. Therefore, based on this observation, when mapping pixel colors to the H-S chart, we assumed the separation would be easily achieved through a supervised classification algorithm such as that offered by BPNN.

For each of the 400 pixels of the 20×20-pixel sample regions, we compute the seven different statistical values that are estimated to reflect the color property of each pixel separately when the surrounding eight pixels also exhibit similar color effects. Table I shows the seven statistical values computed for each pixel.

International Journal of Emerging Technology and Advanced Engineering
Website: www.ijetae.com (ISSN 2250-2459, Volume 2, Issue 5, May 2012)

The values that are generated are collected in a text file. This step is repeated for all the image training zones, Vegetation, Desert, and Road-Streets.

TABLE I
STATISTICAL PROPERTY TAKEN FOR CLASSIFICATION

Pixel Statistical Property	Symbol
Hue Value	H_{HSV}
Saturation Value	S_{HSV}
Intensity Value	V_{HSV}
Standard Deviation for pixel and surrounding 8 pixels (H values)	σ_H
Mean for pixel and surrounding 8 pixels (H values)	AVG_H
Standard Deviation for pixel and surrounding 8 pixels (S values)	σ_S
Mean for pixel and surrounding 8 pixels (S values)	AVG_S

For each pixel that is processed in a 20×20-pixel region, eight pixels surrounding the target pixel are also selected as the candidate points for the average and for the standard deviation computation process. This decision was reached because each pixel is more likely to settle in a class if its neighboring ones are close enough to the same class.

This process continues until all pixels within one sampling color region have been processed. Region after region, we obtain a matrix of 400 rows with 7 columns representing related color properties. In detail, for a single row in a file, the average and standard deviations are registered for each of the H and S color components for each pixel, together with those for the eight surrounding pixels. In addition, the H, S, and V components are inserted in the text file as well. Finally, we obtain a 2-dimensional array that has seven columns: average and standard deviation for the H and S components, and the pixel H, S, and V components.

We chose only 25 sample zones for deserts, 20 for vegetation, and 15 for streets. We decided not to continue training with a larger number of sample images since the vegetation detection results was already satisfactory, as will be shown in the section on experimentation results.

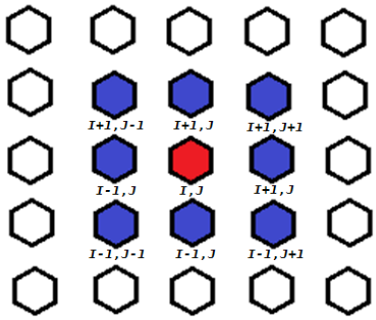

Figure 5. Nine pixel point calculations to generate average and standard deviation. The red pixel and the surrounding eight blue ones are used in calculations of the seven statistical properties of red pixel H-S-V color.

VI. JUSTIFICATIONS FOR USING ROAD-STREET SAMPLES

When only desert and vegetation color samples were considered for input in our MLP network, then the output classification performance indicated that errors in detection or classification of the Roads-Streets regions occurred. Specifically, they were classed as Vegetation, because the Road-Streets regions had never been considered in training. Therefore, to assist in solving the problem of separating Road-Streets from Vegetation, we decided to add the Road-Streets samples as a new class to be identified. When this decision was implemented, the MLP detection was more accurate than in the first experiment when Roads-Streets were not considered in training at all. This can be seen clearly in the Results section of this paper.

VII. BPNN USED IN VEGETATION RECOGNITION

A few of the color zones selected for use must be learned by the MLP network so that it learns non-linearity of color changes. ANN is appropriate for the analysis of nearly any kind of data, irrespective of their statistical properties. Because ANN was successfully applied for extracting vegetation in research studies reported in the literature, ANN was selected as a very useful method for extracting vegetation-type information in complex vegetation mapping problems.

International Journal of Emerging Technology and Advanced Engineering
Website: www.ijetae.com (ISSN 2250-2459, Volume 2, Issue 5, May 2012)

One disadvantage of ANN, however, is that its computation cost can be high, particularly when its architectural network becomes large.

BPNN is a popular learning algorithm based on a gradient descent method that minimizes the square error between the network output and the target output values. The error is consequently propagated back through the weights of the multi layered networks until the desired error threshold is reached.

We considered applying a multi-layer feed forward back propagation neural network to classify colors based on carefully selected templates of previously downloaded images of deserts and vegetation areas from Google Earth, and then training the network in order to classify any new satellite image that is presented. The network parameters are shown in Table 2. The network output is based on two channels, one for the desert class and the other for the vegetation class, each with a value between 0.0 and 1.0.

TABLE III
PARAMETERS FOR NEURAL NETWORK

Type	Feed Forward Back Propagation NN		
Training Function	Levenberg-Marquardt Back propagation		
Layers	3		
Neurons	Layers		
	1st	2nd	3rd
Excitation Function	17	15 (TAN Signal)	2 (LOG Signal)

The MLP network was used here because it is simple to train and its input and output dimensions are easily processed. Here the ANN classifier is used to classify only three zones: Land (mostly deserts and few urban areas), Vegetated areas, and Streets plus Roads. The ANN model has three layers: input, hidden, and output. The input layer encompasses 7 neurons to reflect the 7 statistical properties of the pixel taken, the middle layer has 15 and 20 neurons, while the output layers has only 2 neurons to symbolize the 2 classes needed, one for vegetation alert and the other for land alert on a scale from 0.0 to 1.0 for each.

All the nodes use bilinear sigmoidal functions for their perceptrons, except for the hidden nodes that use a nonlinear sigmoidal function.

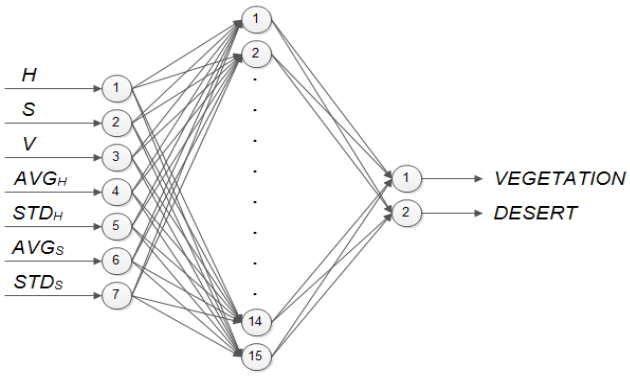

Figure 6. BPNN network used in research with 7 neuron for input layer, 15 neurons for hidden layer, and 2 neurons for output layer.

Window image samples of 20×20 pixels were randomly collected from the multiple images of the surface of Qatar supplied by Google Earth imaging. Between 20 and 25 samples for both land zones and vegetation zones, and only 10 samples for the road-street zone were used at first. When selecting the sample images, we tried to achieve the best possible diversity, and therefore we experimented on different selections of samples. Some selections of the training samples in the early training phases consisted of 5 samples from each category. This number was increased to a selection of 15 samples, and finally nearly 25 to 30 samples were used for each zone. These variations were necessary as each had its advantage in terms of the results.

The number of hidden nodes required to achieve fast convergence was determined during the training procedure. This process started with choosing a small number of neurons. The number was then increased in steps until convergence was reached. It was found that 15 neurons are sufficient to ensure fast conversion.

By translating color from RGB coordinates to HSV coordinates, we succeeded in cancelling the intensity or illumination differences whose source is usually different imaging environments, and hence in separating pure color information from brightness. As MLP is used to register the non-linearity diversity of colors for the three different classes under consideration, it learns the non-linearity relationship between Vegetation and Desert-Road-Street colors.

International Journal of Emerging Technology and Advanced Engineering
Website: www.ijetae.com (ISSN 2250-2459, Volume 2, Issue 5, May 2012)

To learn such non-linearity of color changes efficiently from subject color samples, a large number of color samples are required, as shown in the examples in the next figure.

Finally, the seven calculated properties are injected as an input vector to the trained MLP, and the output, which indicates whether the target pixel belongs to the Vegetation or Desert-Street class, is checked.

We can conclude that a pixel belongs to the Vegetation type or class if the first output bit value is > 0.6 and the second output bit value is < 0.5. Similarly, if the first output value is < 0.5 and the second output value is > 0.6 then it will be considered a Desert or Road-Street pixel.

VIII. Experimentation and Results

The three training phases considered: (1) only vegetation and desert areas; (2) vegetation, desert areas, and roads-streets, with a small number of training samples; and (3) a higher number of training samples, which were carefully selected so that a fast ANN training convergence would be assured.

Fig. 7 shows an original image of an urban area where streets and some manmade vegetation are shown. The figure shows the resultant binary image for the three training phases. Fig. 8 shows scattered vegetation in the middle of deserts when Phase 3 training was applied. The accuracy of the vegetation detection is clear. Fig. 9 shows an urban area with roads and with a small area of vegetation to test the different phases. The top right binary image shows the streets that were detected as vegetation areas in error.

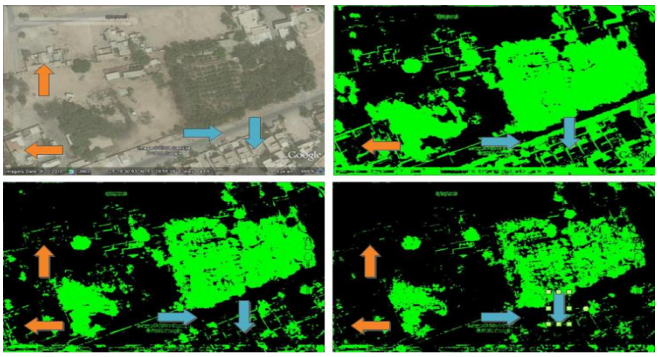

Figure 7. Top left: original image of urban area with manmade vegetation where blue arrows point to roads and houses. Top right: binary image with Phase 1 training where green pixels correspond to vegetation. Bottom left: binary image with Phase 2 training. Bottom right: binary image with Phase 3 training.

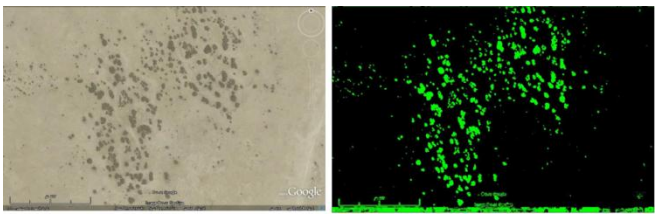

Figure 8. Left: Original image of desert area with scattered vegetation. Right: the binary image shows green pixels that correspond to vegetation with Phase 3 training.

The level of detection error is high when applying Phase 1. The bottom right binary image shows the best result, since almost all the road and street areas have been removed, leaving the small areas of vegetation almost untouched and correctly detected.

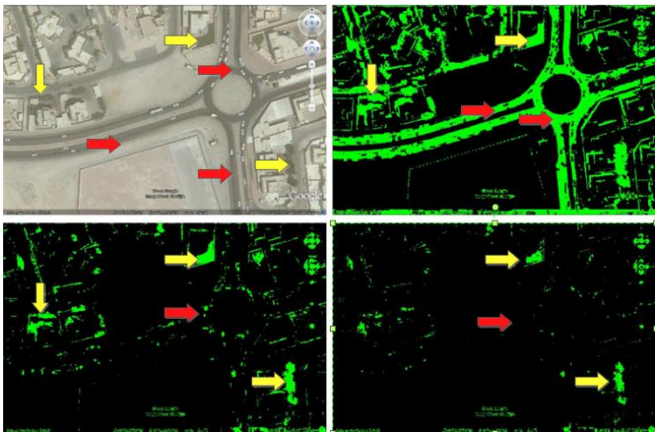

Figure 9. Top left: Original image for urban area with man-made vegetation where blue arrows point to roads and houses. Top right: binary image with Phase 1 training where green pixels correspond to vegetation. Bottom left: binary image with phase 2 training. Bottom right: binary image with Phase 3 training.

IX. Conclusion

We presented an approach for vegetation detection in the desert areas of Qatar that can operate successfully even in high density urban areas. We used the HSV color coordinate, which depends on a high level of averaging and standard deviation calculation for eight pixels surrounding a target pixel to capture well the color nonlinearity of the three classes existing in deserts. BPNN, based on 3 layers of neurons with 15 neurons assigned for the hidden layer, was a useful tool for supervised learning and classification.

The performance of our proposed algorithm was verified by careful inspection of the resulting binary images. However, in some situations it was very difficult for our algorithm to discriminate between urban areas and deserts and between desert and vegetated areas. Nonetheless, this confusion was rare, and the algorithm was shown to be highly dependable in the detection of vegetation in Google Earth images of deserts.

REFERENCES

[1] C. Iovan, D. Boldo, M. Cord, and M. Erikson, 2007 , Automatic extraction and classification of vegetation areas from high resolution images in urban areas, in Proc. 15th Scandinavian Conference on Image Analysis (SCIA'07), p. 858-867.

[2] C. Iovan, D. Boldo, and M. Cord, 2008, Detection, segmentation and characterization of vegetation in high-resolution aerial images for 3D city modeling, International Archives of Photogrammetry, Remote Sensing and Spatial Information Sciences, Vol. 37 (Part 3A), pp.247-252, Pékin, Chine, juillet.

[3] Y. Kim, H. Bae, S. Kim, K. B. Kim, and H. Kang, 2006, Natural color recognition using fuzzification and a neural network for industrial applications, in Proc. Third International Conference on Advances in Neural Networks - Volume Part III (ISNN'06),. p. 991-996.

[4] H. C. Choi, S. Y. Oh, 2010, Illumination invariant lane color recognition by using road color reference & neural networks, in Proc. International Joint Conference on Neural Networks (IJCNN), July 2010, vol., no., pp. 1-5.

[5] A. A. Almhab, and I. Busu, 2008, The approaches for oasis desert vegetation information abstraction based on medium-resolution Lansat TM image: A case study in desert wadi Hadramut Yemen, in Proc. 2008 Second Asia International Conference on Modelling & Simulation (AMS) (AMS '08),. p. 356-360.

[6] E. Youhao, J. Wang, S. Gao, P. Yan, and Z. Yang, 2007, Monitoring of vegetation changes using multi-temporal NDVI in peripheral regions around Minqin oasis, northwest China," Geoscience and Remote Sensing Symposium,. IGARSS 2007. IEEE International, vol., no., pp. 3448-3451, 23-28 July 2007.

[7] Z. Huai-bao, L. Tong, C. Yao-ping, L. Jia-qiang, 4-5 July 2009, Using multi-spectral remote sensing data to extract and analyze the vegetation information in desert Areas, in Proc. International Conference on Environmental Science and Information Application Technology, ESIAT 2009. vol. 3, pp. 697-702.

[8] A. Karnieli, and G. Dall'Olmo, 2003, Remote-sensing monitoring of desertification, phenology, and droughts, Management of Environmental Quality: An International Journal, vol. 14, no. 1, pp. 22 -38.

[9] M.-L. Lin, C.-W. Chen, Q.-B. Wang, Y. Cao, J.-Y. Shih, Y.-T. Lee, C.-Y. Chen, and S. Wang, 2009, Fuzzy model-based assessment and monitoring of desertification using MODIS satellite imagery," Engineering Computations, vol. 26, no. 7, pp. 745 – 760.

[10] X. Yang, G.-M. Jiang, X. Luo, and Z. Zheng, March 2012, Preliminary mapping of high-resolution rural population distribution based on imagery from Google Earth: A case study in the Lake Tai basin, eastern China, Applied Geography, vol. 32, no. 2., pp. 221-227.

[11] Google Earth Pro, WWW. E CONT ENTMAG. COM.